Solar Energy Materials & Solar Cells 157 (2016) 468–475

Contents lists available at ScienceDirect

Solar Energy Materials & Solar Cells

journal homepage: www.elsevier.com/locate/solmat

Efficiency enhancement in solar cells using photon down-conversion in Tb/Yb-doped tellurite glass

Luciano de A. Florêncio [a], Luis A. Gómez-Malagón [a,*], Bismarck C. Lima [b], Anderson S.L. Gomes [b], J.A.M. Garcia [c,d], Luciana R.P. Kassab [c]

[a] University of Pernambuco, Polytechnic School of Pernambuco, 50720-001 Recife, PE, Brazil
[b] Federal University of Pernambuco, Department of Physics, 50670-901 Recife, PE, Brazil
[c] Faculty of Technology of São Paulo, CEETEPS/UNESP, 01124-060 São Paulo, São Paulo, Brazil
[d] Departamento de Engenharia de Sistemas Eletrônicos, Escola Politécnica da Universidade de São Paulo, 05508-010 São Paulo, SP, Brazil

ARTICLE INFO

Article history:
Received 28 March 2016
Received in revised form
16 July 2016
Accepted 17 July 2016
Available online 25 July 2016

Keywords:
Photovoltaic
Solar cell
Down-conversion
Tellurite glasses
Quantum cutting

ABSTRACT

Management of the solar spectrum incident on a solar cell was studied using tellurite glasses doped with Tb^{3+} and Yb^{3+} ions as a cover slip. From the transmittance measurements through the doped glass, a red-shift of the solar spectrum was observed and the mechanisms involved in this phenomena were investigated through the absorption spectra and luminescent measurements. Energy transfer of the UV radiation into VIS and IR radiation was elucidated by analyzing the emission spectra. From the results, the power dependence of the Yb^{3+} IR luminescence on the pumping laser intensity at 482 nm revealed that the energy transfer mechanism involving a virtual state was predominant in these samples. Total quantum efficiency higher than 100% was obtained for the sample co-doped with 1% of Tb^{3+} ions and 5% of Yb^{3+} ions. The efficiency of commercial Silicon and Gallium Phosphide (GaP) solar cells, covered with tellurite glasses doped with Tb^{3+} and Yb^{3+} ions, was measured and compared to the efficiency with an un-doped the cover glass. Efficiency enhancement was observed with a dependence on the rare earth ions concentrations, and the results were attributed to the modification of the spectral profile of the incident radiation in the IR region.

1. Introduction

Solar energy is a renewable source of energy with low negative impact on the environment. Its growing market is driven by the technological improvements and the policies supporting renewable energy sources [1]. Two approaches are usually explored to increase the efficiency: one is based on the search for new materials or techniques that can explore efficiently the photovoltaic effect, and the second one is related to the solar spectrum modification in order to match it with the solar cell spectral efficiency. In the first case, novel materials such as organic solar cells and thin-films technologies were studied and their potentialities were addressed [2,3]. Also, the Multiple Exciton Generation process has been proposed to increase the internal efficiency in more than 100% as demonstrated using quantum dots [4]. Alternative techniques such as the texturization of silicon solar cells, the use of scattering particles, and the improvement of the fabrication process are also exploited to optimize the efficiency of the solar cells [5]. In another approach, the use of different multi-junction configuration is employed in order to efficiently explore the solar spectrum [6]. On the other hand, the degradation of the solar cell due to the incidence of UV radiation is an important detrimental factor that reduces its efficiency. It can be avoided by converting the UV radiation to near of the band gap frequencies of the solar cell, usually in the near infrared [7]. In this last case, the down-conversion and up-conversion processes in photonic materials, particularly those doped with rare earth ions [8], can be used to manage the solar spectrum. An interesting mechanism to be explored using rare earths doped materials is the quantum cutting. In this process, photons of high energy are converted into photons with low energy, which can lead to quantum efficiencies higher than 100%. Then, the main idea is to convert the UV photons of the solar radiation to photons with energies around 1,1 eV, which is the band gap of silicon solar cells. This process will avoid losses due to thermalization and will produce photons that can be used to create more charge carriers [9]. Photon conversion layers have been proposed in the literature to increase the efficiency of solar cells, but the material's optimization is necessary for further development of the photon conversion concept applied to photovoltaics [10].

* Corresponding author.
E-mail address: lagomezma@poli.br (L.A. Gómez-Malagón).

http://dx.doi.org/10.1016/j.solmat.2016.07.024
0927-0248/

Optical properties of glasses doped with Tb^{3+} and Yb^{3+} ions are widely studied in the literature and the results reveal that they are potential candidates for solar cell applications due to their ability to transfer energy from the UV/VIS region to the NIR region [11–18]. However, a few number of papers report the application of these materials to improve the solar cell efficiency [19].

In this work, we study the down conversion process in tellurite glasses doped with Tb^{3+} and Yb^{3+} ions, and explore its application to modify the solar spectrum to increase the efficiency of commercially available silicon and GaP solar cells.

2. Experimental procedure

Samples of tellurite glasses were prepared using $85.0TeO_2-15.0ZnO$ (TZO glass)composition (in wt%) by the melting-quenching technique [20]. The doping species were Tb_4O_7 (1 and 2 wt%) and Yb_2O_3 (5 and 7 wt%). Reagents were melted at 835 °C in a platinum crucible for 1 h, quenched in a pre-heated brass mold, annealed at 325 °C for 2 h, and then cooled to room temperature in the furnace to reduce internal stress. Samples with approximately 3 mm thickness were cut and polished.

Absorption spectra and luminescence measurements were performed to characterize the optical behavior of the samples. The absorption spectra were obtained using a spectrophotometer (Agilent CARY 5000 UV-VIS-NIR) operating in the range of 350–2500 nm. The luminescence measurements were carried out using the third harmonic generation from a 1064 nm pulsed nanosecond Nd: YAG laser (QuantelUltra 50) and an OPA (Coherent Libra) tuned at 482 nm operating in a quasi-continuous (quasi-cw) mode as excitation lasers. The luminescence of the samples was collected using lenses and recorded with a spectrometer (ACTON SP-500i) coupled to a silicon and InGaAs CCD cameras for the VIS and IR measurements, respectively. The temporal measurements were obtained using a Si photodetector (THORLABS PDA100A) attached to a monochromator.

Modification of the solar spectrum was obtained from the measurements of the solar radiation transmittance emitted by a solar simulator (LCS-100 Newport) through the samples using a portable spectrometer (HR4000 Ocean Optics) and a calibrated reference solar cell (91,150 V Newport).

Electrical characterization was performed using a solar simulator (LCS-100 Newport) with a AM 1.5 filter and a sourcemeter (Keithley 2420) coupled to a PC. Efficiency, fill factor (FF), short-circuit current (I_{sc}) and open-circuit voltage (V_{oc}) and the current and voltage (I_{mp}, V_{mp}) at the maximum power were obtained from the Voltage-Current (V-I) curves obtained under 1000 W/m^2 irradiance of commercial silicon (BPW34 Vishay Semiconductors) and GaP (FGAP71 Thorlabs) semiconductors.

3. Results and discussion

The absorption spectra of tellurite glasses doped with 1% and 2% of Tb^{3+} co-doped with 2% and 5% of Yb^{3+} are shown in Fig. 1 (a) and (b). From these figures, the absorption bands corresponding to the $Tb^{3+}$and Yb^{3+}ions excited from the $^7F_6$ and $^2F_{7/2}$ ground states, respectively, are identified and represented in the energy level diagram in Fig. 2. Also, the band gap of the tellurite glass around 380 nm is observed.

In order to understand the role of the UV excitation in the VIS-IR emission, the emission spectra under laser excitation at 355 nm and 482 nm are shown in Figs. 3 and 4, respectively. From these figures, the visible emission in the region of 500 – 700 nm was observed and assigned to the electronic transitions of $^5D_4 \rightarrow {}^7F_j$ (j=6, 5, 4, 3) of Tb^{3+} ions. For the sample prepared with 1% of

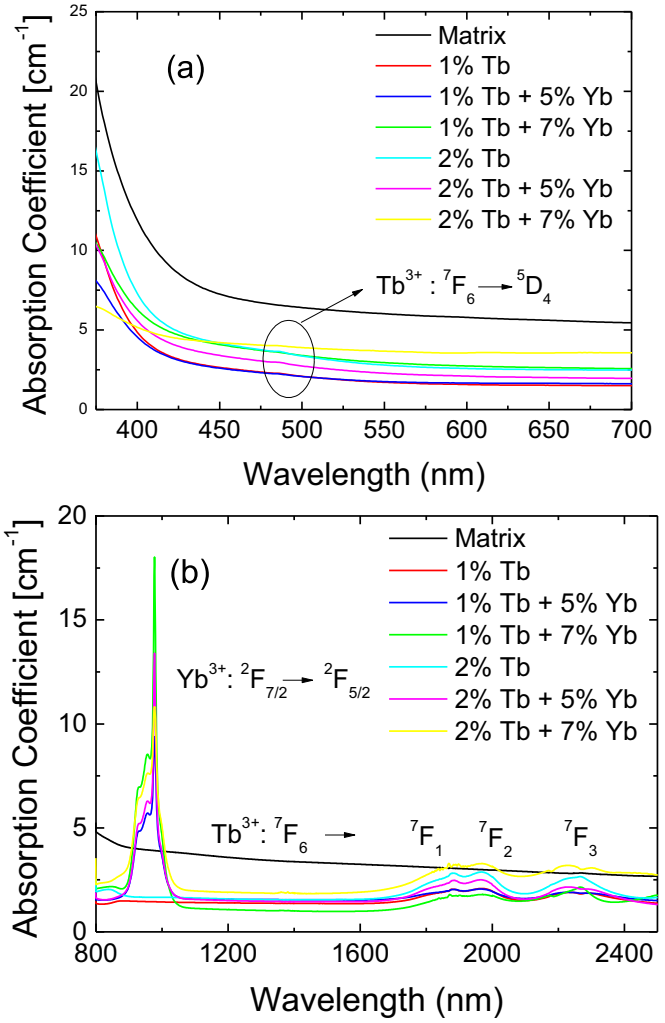

Fig. 1. Absorption spectra of the tellurite glasses doped with 1% and 2% of Tb^{3+} ions and co-doped with 5% and 7% of Yb^{3+} ions. a) VIS spectrum, and b) NIR spectrum.

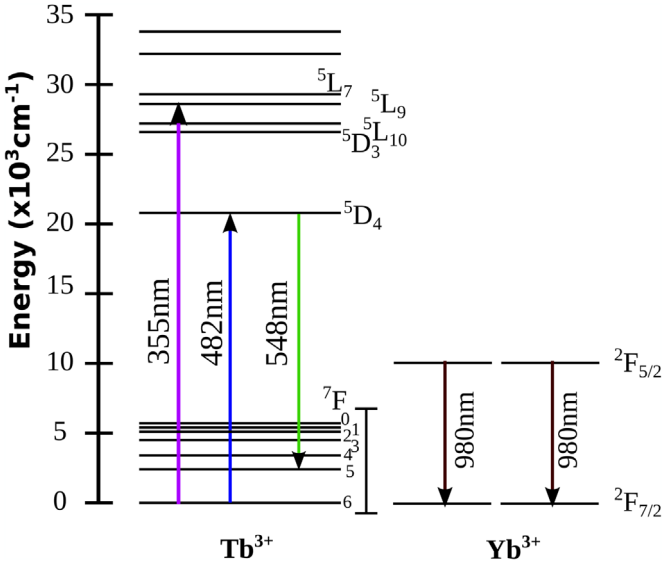

Fig. 2. Diagram of the energy levels of Tb^{3+} and Yb^{3+} ions.

Please cite this article as: L.d.A. Florêncio, et al., Efficiency enhancement in solar cells using photon down-conversion in Tb/Yb-doped tellurite glass, Solar Energy Materials and Solar Cells (2016), http://dx.doi.org/10.1016/j.solmat.2016.07.024

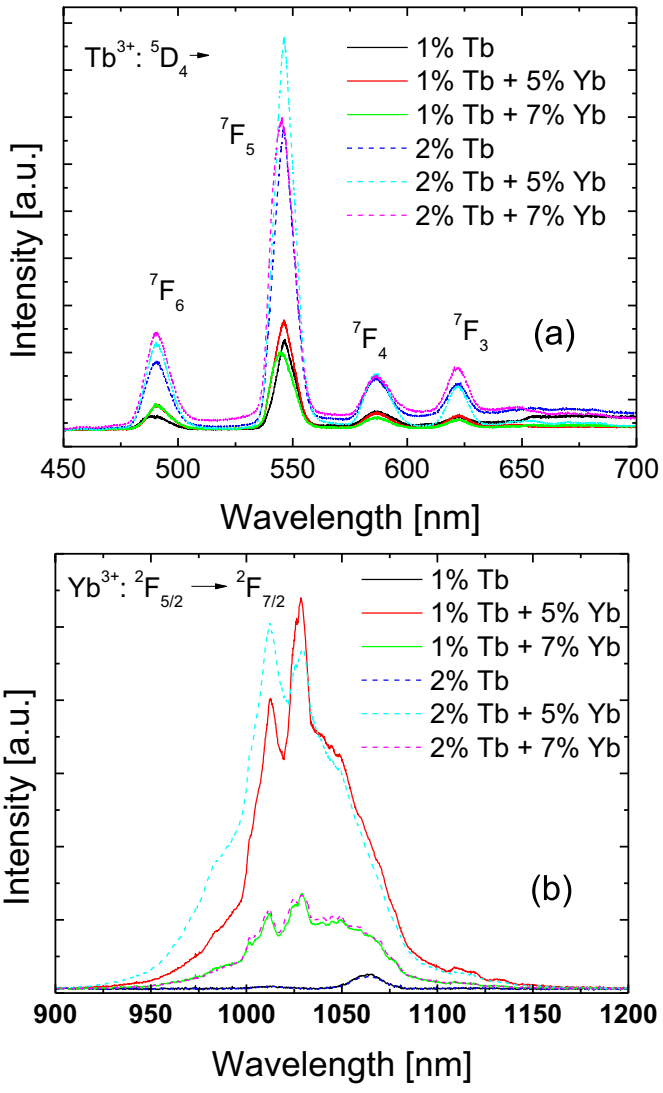

Fig. 3. Emission spectra of tellurite glasses under 355 nm laser excitation. VIS spectra for samples doped with 1% and 2% (a) of Tb^{3+} ions co-doped with 5% and 7% of Yb^{3+} ions. (b) NIR spectrum for samples doped with 1% and 2% of Tb^{3+} and co-doped with 5% and 7% of Yb^{3+} ions.

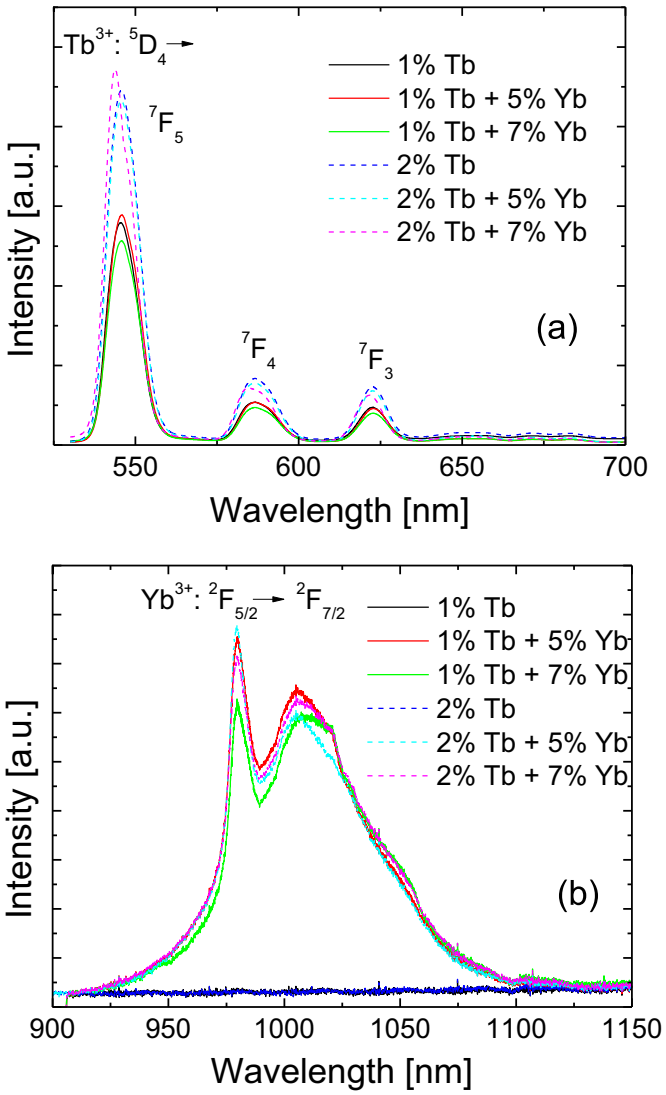

Fig. 4. Emission spectra of tellurite glasses under 482 nm laser excitation. VIS spectra for samples doped with 1% and 2% (a) of Tb^{3+} ions co-doped with 5% and 7% of Yb^{3+} ions. (b) NIR spectrum for samples doped with 1% and 2% of Tb^{3+} ions and codoped with 5% and 7% of Yb^{3+} ions.

Tb^{3+} ion, under excitation at 355 nm, the emission at $^5D_4 \rightarrow {}^7F_5$ (~548 nm) increases when it is co-doped with 5% of Yb^{3+} ion, and decreases when co-doped with 7% of the Yb^{3+} ion. Enhancement of the VIS emission under UV excitation in Tb–Yb systems upon increasing the Yb^{3+}ion concentration has been observed before [11], and is mainly due to the following cross relaxation mechanism: the upper lying states $(Tb)+{}^3F_6(Yb) \rightarrow {}^5D_4(Tb)+{}^2F_{5/2}(Yb)$. Meanwhile, the emission in the IR region increases for the sample co-doped with 5% of the Yb^{3+} ion, and decreases for the one co-doped with 7% of the Yb^{3+} ion, as shown in Fig. 3(b). It indicates that a quenching processes is present for high Yb^{3+} ion concentrations [18]. Similar behavior was observed in the IR region, at 980 nm, for the sample doped with 2% of Tb^{3+} ion excited at 482 nm. The intensity of these emission bands can be attributed to three mechanisms: phonon assisted energy transfer, energy transfer with the participation of a virtual and intermediate metastable state, and cooperative energy transfer (C.E.T.) [12,13], as shown in Fig. 5. Considering that the phonon energy of tellurite glasses is ~700 cm^{-1} [20] and the energy difference between level $^7F_0$ (Tb) and the virtual state level with the same energy of $^2F_{5/2}$ (Yb) is ~4200 cm^{-1}, six phonons are necessary to have a phonon assisted energy transfer. Therefore, the probability to have a multi-phonon relaxation is very low. In order to identify the other energy transfer mechanisms, the dependence of Yb^{3+} ion IR emission on the pumping laser intensity can be analyzed, as it indicates the nature of the process. For a mixed process involving the cooperative energy transfer and the energy transfer through a virtual state, the IR emission from the Yb^{3+} ion is given by [13]:

$$I_{Yb} = \chi\left[\eta\rho^{\frac{1}{2}} + (1-\eta)\rho\right] \quad (1)$$

where χ is the normalization coefficient, ρ is the pump constant and η is the weight given to distinguish the processes. If $\eta=1$, the mechanism is a sub-linear process involving a virtual state. If $\eta=0$, the mechanism is a cooperative energy transfer. To elucidate the mechanism in our samples, the dependence of the IR emission, at 980 nm, on the pump laser intensity at 482 nm is shown in Fig. 6. Using Eq. (1) to fit the experimental data, the values obtained for η vary from 0.87 to 0.89 for samples doped with 2% and 1% of Tb^{3+} ion, respectively. These results show that the contribution of the sub-linear processes is higher than the linear process indicating that the energy transfer involving a virtual state is predominant.

Please cite this article as: L.d.A. Florêncio, et al., Efficiency enhancement in solar cells using photon down-conversion in Tb/Yb-doped tellurite glass, Solar Energy Materials and Solar Cells (2016), http://dx.doi.org/10.1016/j.solmat.2016.07.024

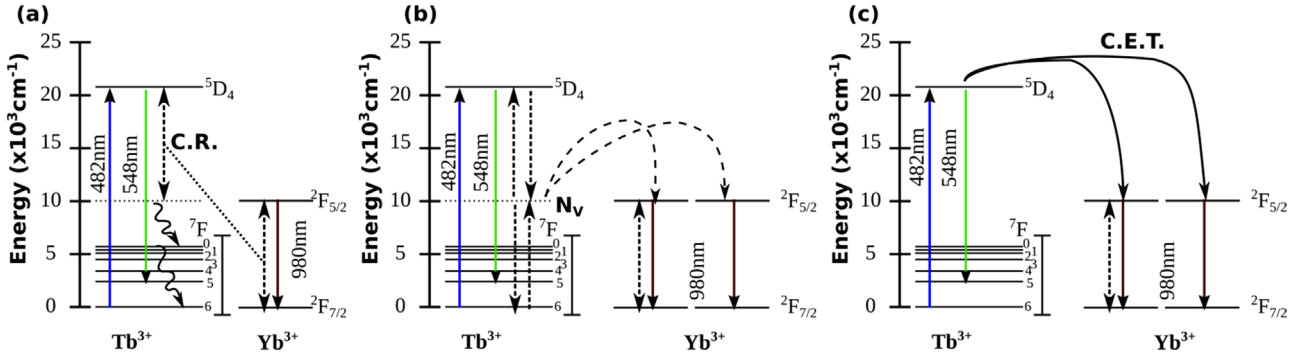

Fig. 5. Energy transfer mechanisms. (a) Phonon assisted energy transfer, (b) energy transfer with the participation of a virtual and intermediate metastable state, and (c) cooperative energy transfer.

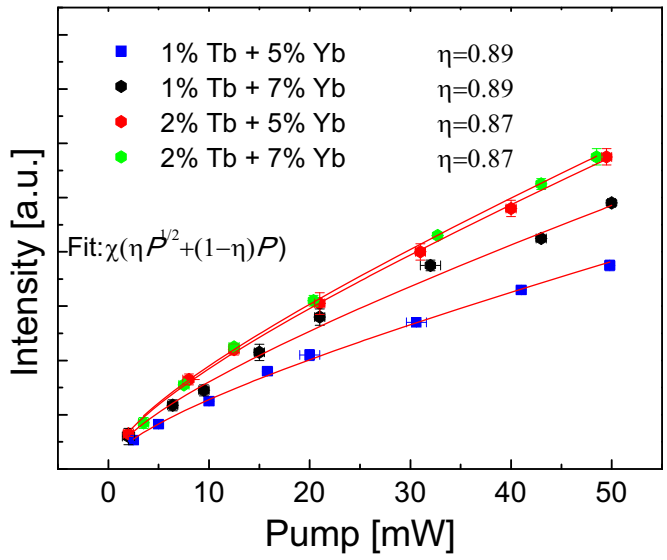

Fig. 6. Power dependence of the IR emission at 980 nm on the laser excitation at 482 nm. The lines show the best fit using Eq. (1).

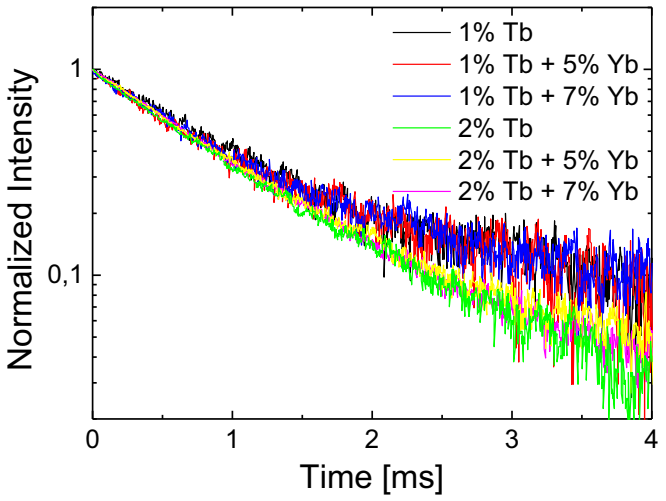

Fig. 7. Temporal behavior of the luminescence at 548 nm under 355 laser excitation.

Defining the energy transfer efficiency, $\eta_{tr,x\%Yb}$, as the ratio of Tb^{3+} ions that depopulates by energy transfer to Yb^{3+} ions over the total number of excited Tb^{3+} ions, and the total quantum efficiency, $\eta_{x\%Yb}$, as the ratio of the emitted to the absorbed number of photons, and considering that all excited Yb^{3+} ions decay radiatively, $\eta_{tr,x\%Yb}$ and $\eta_{x\%Yb}$ can be written as [14]:

$$\eta_{tr,x\%Yb}=1-\frac{\int I_{x\%Yb}dt}{\int I_{0\%Yb}dt} \quad (2)$$

$$\eta_{x\%Yb}=\eta_{Tb}\left(1-\eta_{tr,x\%Yb}\right)+2\eta_{Yb}\eta_{tr,x\%Yb} \quad (3)$$

where η_{Tb} and η_{Yb} are the quantum efficiencies of Tb^{3+} and Yb^{3+} ions, respectively, which were set to be equal to 1. This assumption establishes the high limit of the total quantum efficiency given by (3).

The energy transfer efficiency and the total quantum efficiency were calculated using the average lifetime of the $^5D_4$ level, which is defined as $\tau_m=\int_{t_0}^{\infty} t\,I(t)dt/\int_{t_0}^{\infty} I(t)dt$, where $I(t)$ is the emission intensity at time t_0 after the cutoff of the excitation light. The temporal behavior of the luminescence at ~548 nm under UV excitation is shown in Fig. 7. Results for the energy transfer efficiency and the total quantum efficiency are presented in Table 1. As quenching effects are expected in the sample with higher Yb^{3+} ion concentration, only the sample with 5% of Yb^{3+} ion was considered for the calculation of $\eta_{tr,x\%Yb}$ and $\eta_{x\%Yb}$. A quantum efficiency of ~113% was obtained for the sample doped with 1% of Tb^{3+} and 5% of Yb^{3+}. This result indicates that for 100 photons that are absorbed at 355 nm, 113 photons are produced in the VIS-IR region, of which 26 photons emit at 980–1050 nm region. Similar results were obtained for other hosts containing Tb^{3+} and Yb^{3+} ions [11,15–17,21].

Table 1
Average lifetime of the $^5D_4$ level (τ_m), energy transfer efficiency ($\eta_{tr,x\%Yb}$) and total quantum efficiency ($\eta_{x\%Yb}$) for the studied samples.

Sample	τ_m [ms]	$\eta_{tr,x\%Yb}$	$\eta_{x\%Yb}$
1% Tb	2.52	0	1
1% Tb+5% Yb	2.49	0.127	1.127
2% Tb	1.65	0	1
2% Tb+5% Yb	1.77	1.35×10^{-4}	1.000

The solar spectrum has components in the UV-VIS-NIR region and its interaction with the tellurite glasses doped with Tb^{3+} and Yb^{3+} modifies the solar spectrum. This change was studied through the transmitted irradiance spectra shown in Fig. 8. From this figure, a downshift on the spectra in the 400–800 nm range and the reduction of the UV radiation are observed. These effects were attributed to down-conversion mechanism studied previously and to the absorption of the tellurite glass, respectively. On the other hand, the expected increase of the radiation in the 900–

Please cite this article as: L.d.A. Florêncio, et al., Efficiency enhancement in solar cells using photon down-conversion in Tb/Yb-doped tellurite glass, Solar Energy Materials and Solar Cells (2016), http://dx.doi.org/10.1016/j.solmat.2016.07.024

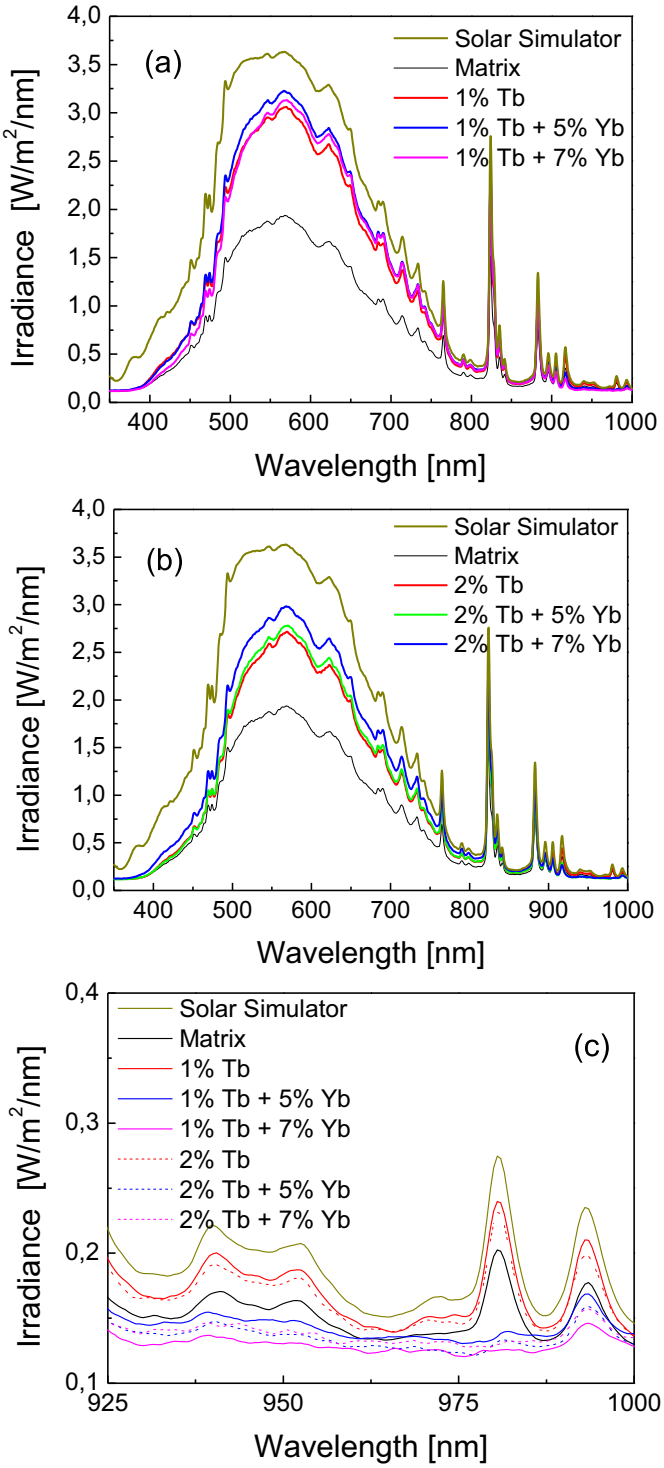

Fig. 8. Transmitted irradiance spectra for (a) samples doped with 1% of Tb^{3+} and (b) 2% of Tb^{3+} ions. IR spectra for all samples (c). The concentration of Yb^{3+} ions was 5% and 7%.

1100 nm region was not observed, indicating that the interplay between the self-absorption of the Yb^{3+} ion and the energy transfer process between the Tb^{3+} and Yb^{3+} ions must be improved.

Voltage-Current (V-I) curves for silicon and GaP solar cells covered with tellurite glasses doped with Tb^{3+} and Yb^{3+} were obtained using the experimental setup represented in Fig. 9, and the results are shown in Figs. 10 and 11, respectively.

From these results, the short-circuit current (I_{sc}), the open-circuit voltage (V_{oc}), the filling factor ($FF=V_{mp}I_{mp}/V_{oc}I_{sc}$) and the efficiency ($eff=V_{oc}I_{sc}FF/A\,I$) were obtained and are shown in Table 2, where A is the cell area and I is the incident irradiance (1000 W/m^2).

It is important to note that the antireflection coating applied on the front surface of the solar cell can affect its performance [22]. Then, it is expected that tellurite glass-covered solar cells will have different efficiencies than the naked solar cell. For this reason, only the efficiencies of solar cells covered with glasses un-doped and doped with rare earths were compared. In this way, we also take into account the glass reflection (within the limit of the glass imperfections).

For silicon solar cells ($E_g=1{,}1$ eV) the efficiency increases for the sample covered with the tellurite glass doped with 1% of Tb^{3+} ion, and decreases with the increase of the Yb^{3+} ion concentration. A decrease of the UV-VIS radiation and an increase of the IR emission is expected when the Yb^{3+} ion concentration increases. This process should increase the efficiency of the solar cells. However, the self-absorption processes and the energy transfer between the Yb^{3+} ions can reduce the transmission at IR wavelength. This can be attributed to the strong correlation of the efficiency with the energy transfer mechanism, explained above for the Tb^{3+} and Yb^{3+} ions. From these results, efficiency enhancement of ~7% was observed for the sample doped only with 1% of Tb^{3+} ions, when compared with the un-doped one. To the best of our knowledge, it is the highest enhancement reported for silicon solar cells using glasses doped with Tb^{3+}/Yb^{3+} ions to manage the solar spectrum. For comparison, a lower enhancement of 0.34% for phosphate glasses co-doped with 1% of Tb^{3+} and 0,5% of Yb^{3+} ions was recently reported [19].

In order to establish a direct one-to-one correlation between the measured spectral changes of the solar spectrum and the reported increase of solar cell efficiency, the software PC1D was used to simulate the V-I curve of a silicon solar cell. This software is widely used to simulate the performance of solar cells and enables the change of the solar cell illumination spectral profile [23,24]. From the simulation, short-circuit current, open-circuit voltage, maximum power and efficiency were determined and the results are shown in Table 3. These results reveal that the efficiency is directly correlated with the overall intensity.

However, experimental results diverge from the simulation. For the samples doped with 1% of Tb^{3+} and 5% of Yb^{3+} and 1% of Tb^{3+} and 7% of Yb^{3+}, the efficiency has a maximum for the sample without Yb^{3+} ion and decreases for samples doped with Yb^{3+} ion as shown in Table 2. The same behavior is observed for the samples doped with 2% of Tb^{3+} and the highest efficiency is observed for the sample doped with 1% of Tb^{3+}. A similar behavior is observed for the transmitted irradiance in the IR spectra as shown in Fig. 8(c). The IR radiation is quenched when the Yb^{3+} concentration is increased. These results suggest that the efficiency of silicon solar cells is strongly affected by the spectral profile of the incident radiation in the IR region.

For GaP solar cells ($E_g=2{,}26$ eV), the modified solar spectrum is partially used in the photovoltaic process. Photons with energies below 2.26 eV are not absorbed. From the results shown in Table 2, it is observed that with the increase of the Tb^{3+} ion concentration, the efficiency is decreased when compared with the one of the un-doped sample. This can be attributed to the quenching of the emission from the $^5D_3$ excited level by cross relaxation ($^5D_3+{}^7F_6\rightarrow{}^5D_4+{}^7F_0$) and multiphonon relaxation [21]. Also, for the samples doped with 1% of Tb^{3+}, the efficiency has a maximum for the sample co-doped with 5% of Yb^{3+} and decreases for the sample co-doped with 7% of Yb^{3+}. In the case of the samples doped with 2% of Tb^{3+}, the efficiency increases with the Yb^{3+} concentration, up to 5% of Yb^{3+}, and decreases for the sample co-

Please cite this article as: L.d.A. Florêncio, et al., Efficiency enhancement in solar cells using photon down-conversion in Tb/Yb-doped tellurite glass, Solar Energy Materials and Solar Cells (2016), http://dx.doi.org/10.1016/j.solmat.2016.07.024

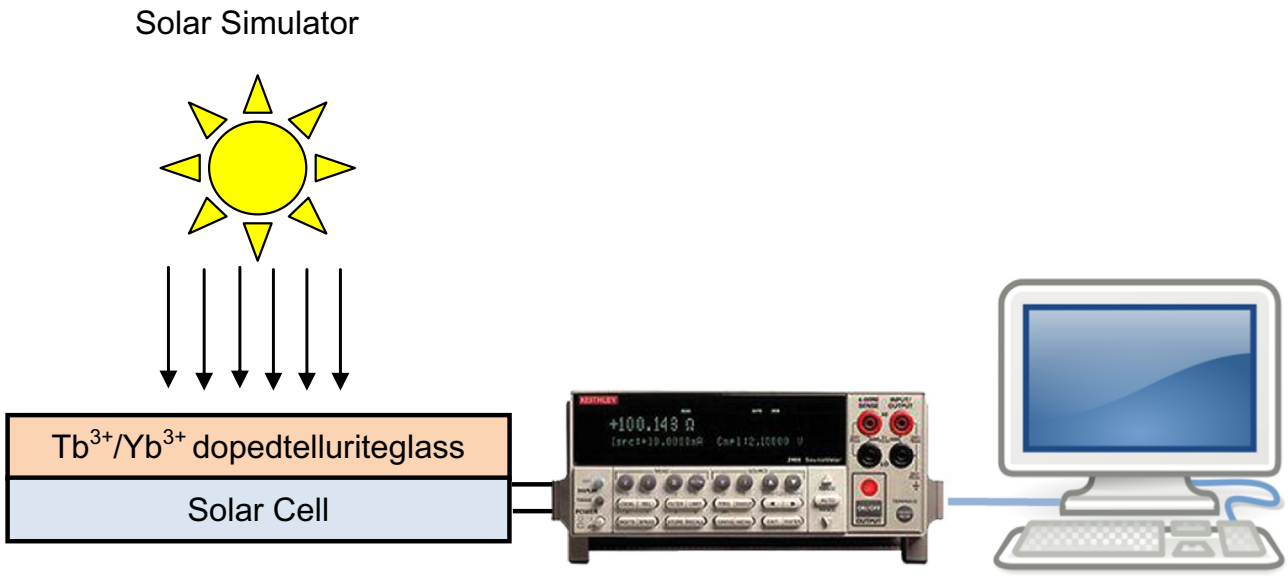

Fig. 9. Experimental setup for the electrical characterization of Tb^{3+}/Yb^{3+} ions doped tellurite glasses.

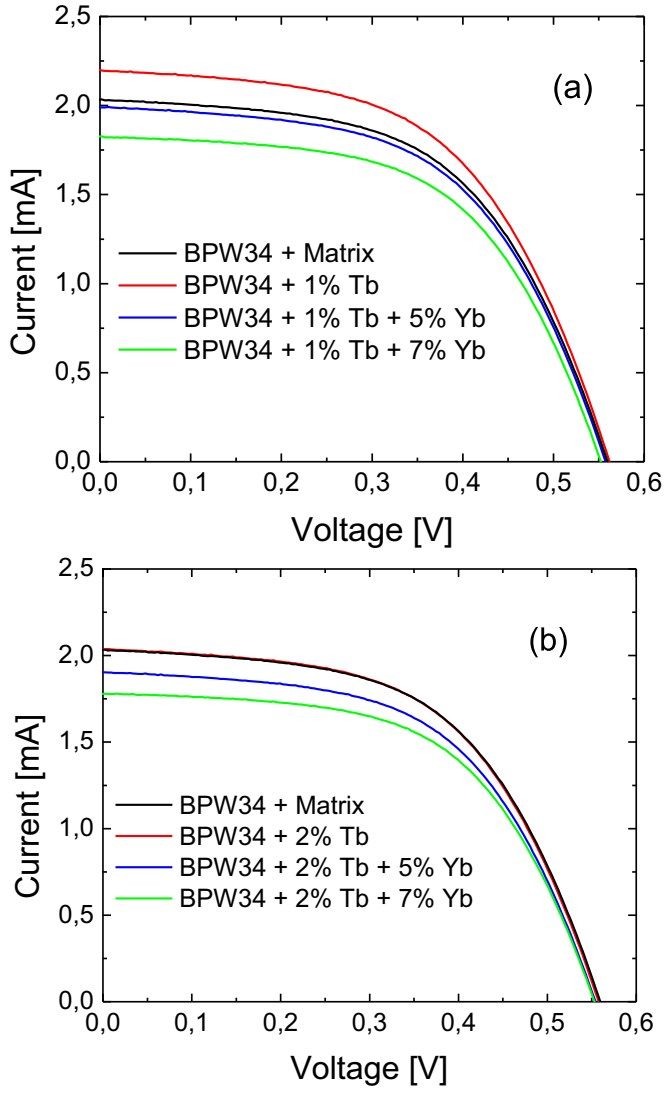

Fig. 10. V-I curves for the BPW34 solar cell covered with tellurite glass doped with (a) 1% of Tb^{3+} and (b) 2% of Tb^{3+} ions. The concentration of Yb^{3+} ions was 5% and 7%.

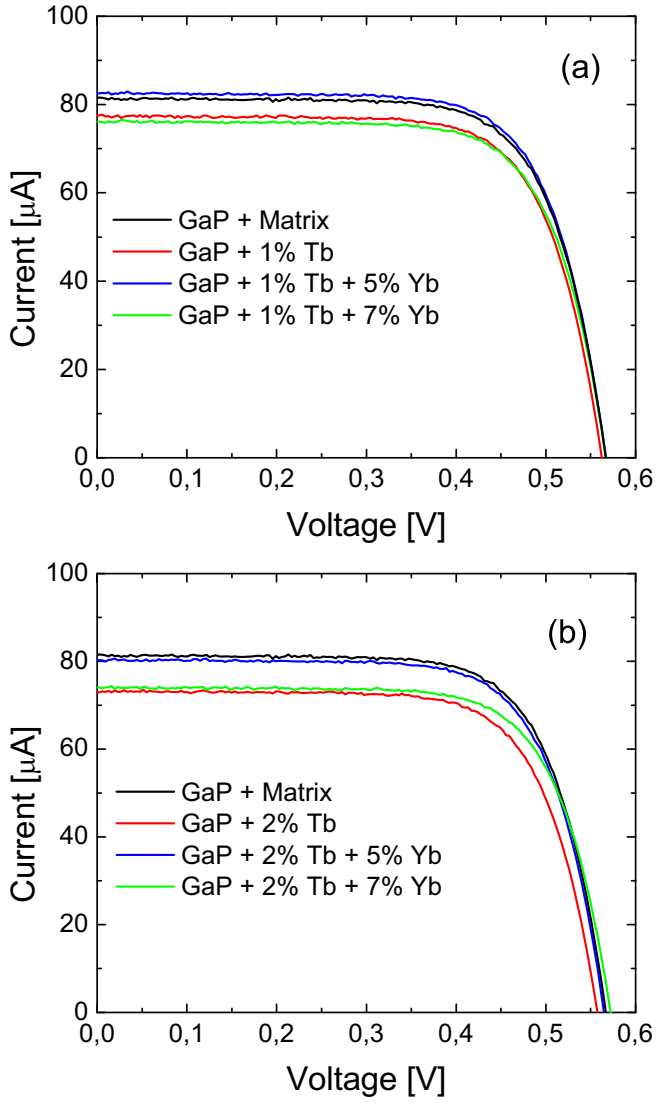

Fig. 11. V-I curves for the GaP solar cell covered with tellurite glass doped with (a) 1% of Tb^{3+} and (b) 2% of Tb^{3+} ions. The concentration of Yb^{3+} ions was 5% and 7%.

Please cite this article as: L.d.A. Florêncio, et al., Efficiency enhancement in solar cells using photon down-conversion in Tb/Yb-doped tellurite glass, Solar Energy Materials and Solar Cells (2016), http://dx.doi.org/10.1016/j.solmat.2016.07.024

Table 2
Electrical parameters (I_{sc} and V_{oc}), filling factor (FF) and efficiencies of the studied samples. Uncertainty in efficiency calculation is ± 0.00001.

Solar cell	Matrix doping [%]		I_{sc} (10^{-5}) [A]	V_{oc} [V]	FF	Efficiency [%]
	Tb	Yb				
BPW34	0	0	203	0.55778	0.5550	6.9818
BPW34	1	0	220	0.56136	0.5443	7.4692
BPW34	1	5	196	0.5542	0.5643	6.8110
BPW34	1	7	183	0.55076	0.5647	6.3237
BPW34	2	0	197	0.55419	0.5737	6.9597
BPW34	2	5	190	0.55072	0.5607	6.5184
BPW34	2	7	197	0.55077	0.5187	6.2527
GaP	0	0	8.16	0.56481	0.7194	0.6906
GaP	1	0	7.76	0.56126	0.7170	0.6504
GaP	1	5	8.25	0.56474	0.7193	0.6985
GaP	1	7	7.61	0.56487	0.7235	0.6480
GaP	2	0	7.29	0.55429	0.7215	0.6077
GaP	2	5	8.03	0.56481	0.7194	0.6794
GaP	2	7	7.41	0.57179	0.7194	0.6349

Table 3
Electrical parameters (I_{sc}, V_{oc} and P_{max}) and efficiencies obtained for a silicon solar cells simulated with the PC1D software using the transmitted irradiance spectra from Fig. 8.

Matrix doping [%]		I_{sc} (10^{-3}) [A]	V_{oc} [V]	P_{max} (10^{-4}) [W]	Intensity [W/m^2]	Efficiency [%]
Tb	Yb					
0	0	1.49	0.5976	5.82	514	6.47
1	0	2.23	0.6089	8.45	764	9.39
1	5	2.34	0.6103	8.83	801	9.81
1	7	2.26	0.6093	8.56	767	9.51
2	0	1.99	0.6057	7.64	675	8.49
2	5	2.02	0.6062	7.76	686	8.62
2	7	2.21	0.6087	8.42	756	9.35

doped with 7% of Yb^{3+}. The same behavior is observed for the down-converted spectral components near to the band gap under UV excitation, as shown in Fig. 3(a). These results suggest that, as in the case of silicon solar cells, the GaP solar cell efficiency is sensitive to the spectral components of the incident radiation near to the band gap. Enhancement of the efficiency in ~1.1% was observed for the sample co-doped with 1% of Tb^{3+} and 5% of Yb^{3+} ions, when compared with the un-doped one.

4. Conclusion

The spectroscopic analysis of the tellurite (TeO_2–ZnO)glasses doped with Tb^{3+} and Yb^{3+} reveals that under UV radiation that the photon down-conversion is due to a sub-linear process involving a virtual level, and its total quantum efficiency is higher than 100% for the sample co-doped with 1% of Tb^{3+} and 5% of Yb^{3+}.

The efficiency of a commercial solar cell of silicon covered with a tellurite based glass was increased by ~7% when the glass was doped with 1% of Tb^{3+}, as compared to an un-doped glass as the cover top. For the case of a commercial GaP solar cell, efficiency enhancement of ~1.1% was observed when covered with the same tellurite glass, but co-doped with 1% of Tb^{3+} and 5% of Yb^{3+} as compared to an un-doped tellurite glass cover. These results suggest that the efficiency is sensitive to the spectral components of the incident radiation on the solar cell near to the band gap. Moreover, the experiments shown here reveal that the management of Tb^{3+} and Yb^{3+} ions concentration can be optimized to modify the solar spectrum aiming the increase of the solar cells efficiency.

Acknowledgments

The authors would like to acknowledge the Brazilian agencies Conselho Nacional de Desenvolvimento Científico e Tecnológico (CNPq) (Grant number CT Energ 49/2013), Fundacão de Amparo à Ciência e Tecnologia do Estado de Pernambuco (FACEPE) (Grant number Pronex 10/2014) and Escola Politécnica de Pernambuco (POLI–UPE) for financial support. This work was performed under the PRONEX and CNPq (CT Energ 49/2013) Project. The authors also acknowledge Renan Gonçalves for the samples preparation.

References

[1] C. Sener, V. Fthenakis, Energy policy and financing options to achieve solar energy grid penetration targets: accounting for external costs, Renew. Sustain. Energy Rev. 32 (2014) 854–868, http://dx.doi.org/10.1016/j.rser.2014.01.030.
[2] N. Kaur, M. Singh, D. Pathak, T. Wagner, J.M. Nunzi, Organic materials for photovoltaic applications: review and mechanism, Synth. Met. 190 (2014) 20–26, http://dx.doi.org/10.1016/j.synthmet.2014.01.022.
[3] L. Yu, R.S. Kokenyesi, D.A. Keszler, A. Zunger, Inverse design of high absorption thin-film photovoltaic materials, Adv. Energy Mater. 3 (2013) 43–48, http://dx.doi.org/10.1002/aenm.201200538.
[4] R.J. Ellingson, M.C. Beard, J.C. Johnson, P. Yu, O.I. Micic, A.J. Nozik, et al., Highly efficient multiple exciton generation in colloidal PbSe and PbS quantum dots, Nano Lett. 5 (2005) 865–871, http://dx.doi.org/10.1021/nl0502672.
[5] K. Tsujino, M. Matsumura, Y. Nishimoto, Texturization of multicrystalline silicon wafers for solar cells by chemical treatment using metallic catalyst, Sol. Energy Mater. Sol. Cells 90 (2006) 100–110, http://dx.doi.org/10.1016/j.solmat.2005.02.019.
[6] R.R. King, D.C. Law, K.M. Edmondson, C.M. Fetzer, G.S. Kinsey, H. Yoon, et al., 40% efficient metamorphic GaInP/GaInAs/Ge multijunction solar cells, Appl. Phys. Lett. 90 (2007) 183516, http://dx.doi.org/10.1063/1.2734507.
[7] E.L. Meyer, E.E. van Dyk, Assessing the reliability and degradation of photovoltaic module performance parameters, IEEE Trans. Reliab. 53 (2004) 83–92, http://dx.doi.org/10.1109/TR.2004.824831.
[8] H. Lian, Z. Hou, M. Shang, D. Geng, Y. Zhang, J. Lin, Rare earth ions doped phosphors for improving efficiencies of solar cells, Energy 57 (2013) 270–283, http://dx.doi.org/10.1016/j.energy.2013.05.019.
[9] T. Trupke, M.A. Green, P. Würfel, Improving solar cell efficiencies by down-conversion of high-energy photons, J. Appl. Phys. 92 (2002) 1668, http://dx.doi.org/10.1063/1.1492021.
[10] T. Fix, G. Ferblantier, H. Rinnert, A. Slaoui, Evaluation of the effective quantum efficiency of photon conversion layers placed on solar cells, Sol. Energy Mater. Sol. Cells 132 (2015) 191–195, http://dx.doi.org/10.1016/j.solmat.2014.09.009.
[11] I.A.A. Terra, L.J. Borrero-González, J.M. Carvalho, M.C. Terrile, M.C.F.C. Felinto, H.F. Brito, et al., Spectroscopic properties and quantum cutting in Tb^{3+}–Yb^{3+} co-doped ZrO_2 nanocrystals, J. Appl. Phys. 113 (2013) 073105, http://dx.doi.org/10.1063/1.4792743.
[12] I.A.A. Terra, L.J. Borrero-González, T.R. Figueredo, J.M.P. Almeida, A. C. Hernandes, L.A.O. Nunes, et al., Down-conversion process in Tb^{3+}–Yb^{3+} co-doped Calibo glasses, J. Lumin. 132 (2012) 1678–1682, http://dx.doi.org/10.1016/j.jlumin.2012.02.019.
[13] Q. Duan, F. Qin, Z. Zhang, W. Cao, Quantum cutting mechanism in NaYF_4: Tb^{3+},Yb^{3+}, Opt. Lett. 37 (2012) 521, http://dx.doi.org/10.1364/OL.37.000521.
[14] P. Vergeer, T.J.H. Vlugt, M.H.F. Kox, M.I. den Hertog, J.P.J.M. van der Eerden, A. Meijerink, Quantum cutting by cooperative energy transfer in $Yb_xY_{1-x}PO_4$: Tb^{3+}, Phys. Rev. B. 71 (2005) 014119, http://dx.doi.org/10.1103/PhysRevB.71.014119.
[15] Y. Wang, L. Xie, H. Zhang, Cooperative near-infrared quantum cutting in Tb [sup3+], Yb[sup3+] codoped polyborates La[sub0.99−x]Yb[subx]BaB[sub9]O [sub16]:Tb[sub0.01], J. Appl. Phys. 105 (2009) 023528, http://dx.doi.org/10.1063/1.3056382.
[16] Q.Y. Zhang, C.H. Yang, Z.H. Jiang, X.H. Ji, Concentration-dependent near-infrared quantum cutting in GdBO[sub3]:Tb[sup3+], Yb[sup3+] nanophosphors, Appl. Phys. Lett. 90 (2007) 061914, http://dx.doi.org/10.1063/1.2472195.
[17] L. Zhao, D. Wang, Y. Wang, Y. Tao, Visible quantum cutting and energy transfer in Tb^{3+}-doped KSr(Gd,Y)(PO4)2 under VUV-UV excitation, J. Am. Ceram. Soc. 97 (2014) 3913–3917, http://dx.doi.org/10.1111/jace.13235.
[18] X. Zhou, Y. Wang, G. Wang, L. Li, K. Zhou, Q. Li, Cooperative down-conversion and near-infrared luminescence of Tb^{3+}/Yb^{3+} co-doped tellurite glass, J. Alloy. Compd. 579 (2013) 27–30, http://dx.doi.org/10.1016/j.jallcom.2013.05.058.
[19] G. Li, C. Zhang, P. Song, P. Zhu, K. Zhu, J. He, Luminescence properties in Tb^{3+}/Yb^{3+} codoped phosphate glasses for solar cells, J. Alloy. Compd. 662 (2016)

89–93, http://dx.doi.org/10.1016/j.jallcom.2015.12.074.
[20] L.R.P. Kassab, L.F. Freitas, T.A.A. Assumpção, D.M. da Silva, C.B. de Araújo, Frequency upconversion properties of Ag:TeO_2–ZnO nanocomposites codoped with Yb^{3+} and Tm^{3+} ions, Appl. Phys. B 104 (2011) 1029–1034, http://dx.doi.org/10.1007/s00340-011-4451-1.
[21] M. Xie, Y. Tao, Y. Huang, H. Liang, Q. Su, The Quantum cutting of Tb^{3+} in $Ca_6Ln_2Na_2$ $(PO_4)6F2$ (Ln=Gd, La) under VUV-UV excitation: with and without Gd^{3+}, Inorg. Chem. 49 (2010) 11317–11324, http://dx.doi.org/10.1021/ic101028n.
[22] U. Sikder, M.A. Zaman, Optimization of multilayer antireflection coating for photovoltaic applications, Opt. Laser Technol. 79 (2016) 88–94, http://dx.doi.org/10.1016/j.optlastec.2015.11.011.
[23] P.A. Basore, D.A. Clugston, PC1d Version 5.9, 2003. ⟨https://www.engineering.unsw.edu.au/energy-engineering/pc1d-software-for-modelling-a-solar-cell⟩).
[24] D.A. Clugston, P.A. Basore, PC1D version 5: 32-bit solar cell modeling on personal computers, in: Proceedings of the Photovolt. Spec. Conf. 1997, Conf. Rec. Twenty-Sixth IEEE, 1997, pp. 207–210, http://dx.doi.org/10.1109/PVSC.1997.654065.

Please cite this article as: L.d.A. Florêncio, et al., Efficiency enhancement in solar cells using photon down-conversion in Tb/Yb-doped tellurite glass, Solar Energy Materials and Solar Cells (2016), http://dx.doi.org/10.1016/j.solmat.2016.07.024